

Organocobalt Mediated Radical Polymerization of Acrylic Acid in Water

Chi-How Peng, Michael Fryd, and Bradford B. Wayland*

Department of Chemistry, University of Pennsylvania, Philadelphia, Pennsylvania 19104-6323

Received April 9, 2007; Revised Manuscript Received July 9, 2007

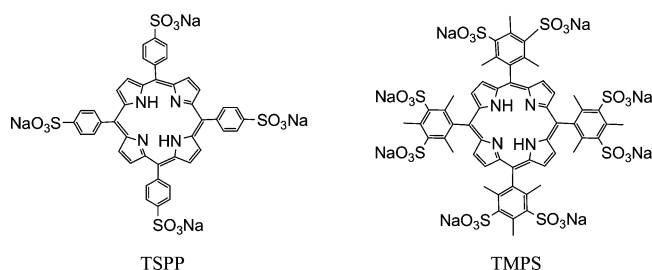
ABSTRACT: Low polydispersity high molecular weight poly(acrylic acid) (PAA) is formed rapidly by the aqueous polymerization of acrylic acid (AA) initiated by an azo radical source (V-70) in the presence of cobalt complexes of tetra(3,5-disulfonatomesityl) porphyrin. Water-soluble cobalt(II) porphyrins in conjunction with an azo radical source and acrylic acid react to produce organocobalt complexes that mediate the radical polymerization of AA in water. Linear increase in number-average molecular weight with monomer conversion indicates the living character of the polymerization. Kinetic–mechanistic studies demonstrate that organocobalt complexes mediate the living radical polymerization by both a degenerative transfer radical interchange polymerization (RIP) mechanism and cobalt(II) stable free radical reversible termination.

Introduction

Development of successful approaches for living radical polymerization (LRP) provides routes to a vast array of new low polydispersity (PDI) homo and block copolymers.^{1–20} Many of these polymeric materials are amphiphilic block copolymers prepared from functionalized monomers that can only be polymerized by radical pathways. Formation of low polydispersity high molecular weight acrylic acid (AA) polymers remains a challenge. The incompatibility of acrylic acid with transition metal atom transfer radical polymerization (ATRP) catalysts results in uncontrolled polymerization.²¹ Controlled polymerization of AA can be accomplished by reversible addition fragmentation chain transfer (RAFT)^{7,22,23} and nitroxide mediated polymerization (NMP),^{24,25} but the polymer molecular weights have been limited by chain transfer and other side reactions.

We have recently reported that cobalt porphyrin derivatives can control LRP of acrylate monomers by both a cobalt(II) stable free radical reversible termination mechanism and a much faster and more versatile organocobalt mediated degenerative transfer pathway called radical interchange polymerization (RIP).²⁶ The robust nature of cobalt porphyrins make these catalysts potential candidates for applications with difficult monomers like acrylic acid.

Phenyl-sulfonated porphyrins provide a series of water-soluble cobalt(II) metalloradical and organocobalt complexes for controlling LRP in aqueous media. This article reports on the



application of cobalt porphyrin derivatives in mediating living radical polymerizations of acrylic acid in water that produce high molecular weight low polydispersity poly(acrylic acid)

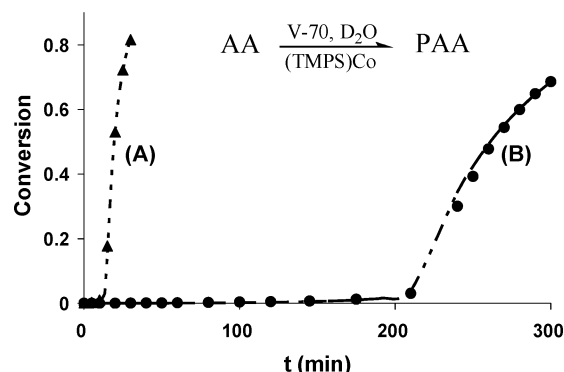


Figure 1. Monomer conversion as a function of time in the radical polymerization of acrylic acid (4.72 M) initiated by V-70 (1.68×10^{-3} M) in D_2O at (A) 333 K [with $[(\text{TMPS})\text{Co}^{\text{II}}]_i = 1.30 \times 10^{-3}$ M; conversion = 81.6%; $M_n = 232\,000$ (theory 212 000); $M_w/M_n = 1.20$] and (B) 313 K [with $[(\text{TMPS})\text{Co}^{\text{II}}]_i = 1.24 \times 10^{-3}$ M; conversion = 68.6%; $M_n = 195\,000$ (theory 187 000); $M_w/M_n = 1.33$]. The lines are simulated results using rate constants given in the experimental section.

(PAA) and kinetic–mechanistic studies of the polymerization process.

Results and Discussion

Representative monomer conversion vs time plots for the radical polymerizations of acrylic acid (AA) in water (333 K) using an azo radical source (V-70) in the presence of cobalt tetra(3,5-disulfonatomesityl)porphyrin ((TMPS)Co^{II}) are shown in Figure 1 and first-order rate plots are illustrated in Figures 2 and 3. The polymerization process involves an induction period where only a small amount of polymer forms followed by a stage of relatively fast polymerization (Figures 1–3). Radical polymerization of AA in the presence of (TMPS)Co^{II} at 333 K where $t_{1/2}$ (V-70) is only 10.2 min²⁷ (Figure 1A) proceeds to 81.6% conversion, producing poly(acrylic acid) (PAA) with an number-average molecular weight (M_n) of 232 000 (theory 212 000) and polydispersity of 1.20 in a total time of 30 min which includes a 13 min induction period. Carrying out the AA polymerization at 313 K where $t_{1/2}$ (V-70) is 142 min²⁷ (Figure 1B) extends the induction period to 213 min and at 68.6% conversion produces PAA with an M_n of 195 000 (theory 187 000) and polydispersity of 1.33. The measured M_n values are close to the theoretical values based on one living chain per cobalt porphyrin. The observed conversion vs time plots

* Corresponding author. E-mail: wayland@sas.upenn.edu.

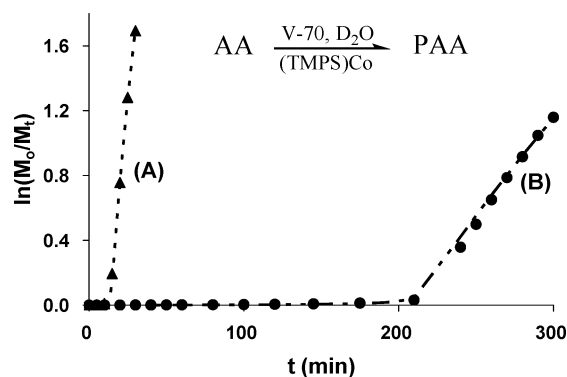


Figure 2. Kinetic plots for polymerization of acrylic acid (4.72 M) in D_2O at 313 K and 333 K initiated by V-70 (1.68×10^{-3} M): (A) 333 K $[(TMPS)Co^{II}]_i = 1.30 \times 10^{-3}$ M; conversion = 81.6%; $M_n = 232\,000$ (theory 212 000); $M_w/M_n = 1.2$; (B) 313 K $[(TMPS)Co^{II}]_i = 1.24 \times 10^{-3}$ M; conversion = 68.6%; $M_n = 195\,000$ (theory 187 000); $M_w/M_n = 1.33$. Dashed lines are calculated using kinetic parameters given in the Experimental Section.

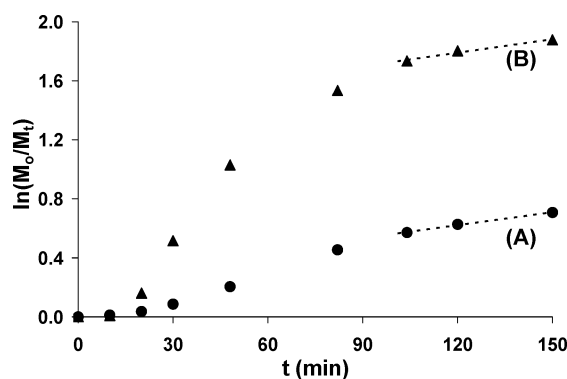


Figure 3. Kinetic plots for polymerization of acrylic acid (AA) in D_2O at 333 K with $[(TMPS)Co^{II}]_i = 1.82 \times 10^{-3}$ M, $[V-70]/[(TMPS)Co^{II}]_i = 1.30$, and two concentrations of $[AA]_i$: (A) $[AA]_i = 1.00$ M [conversion = 50.7%; $M_n = 18\,000$ (theory 20 000); $M_w/M_n = 1.41$]; (B) $[AA]_i = 2.50$ M [conversion = 84.7%; $M_n = 77\,000$ (theory 84 000); $M_w/M_n = 1.38$].

(Figure 1) and first-order kinetic plots (Figure 2) are simulated by using experimental rate constants for radicals entering solution from V-70, propagation constants for AA,²⁸ equilibrium constants for dissociation of $(TMPS)Co-PAA$ and allowing the effective radical termination constant to vary to obtain the best fit (Experimental Section). The induction periods shown in Figure 1 correspond accurately with the time required for V-70 to inject one radical into solution for each $(por)Co^{II}$ molecule.

First-order rate plots in Figures 2 and 3 along with kinetic simulations show that the rate of polymerization after the induction period increases rapidly to values that are determined by the concentration of V-70 as the radical source. When the external radical source (V-70) is exhausted, after a period of 90 min at 333 K, the polymerization rate decreases because dissociation of organocobalt complex $((por)Co-PAA)$ becomes the exclusive radical source, which is one of the features of a reversible termination LRP. The radicals in solutions are maintained at low concentration by quasi-equilibrium with the dormant organocobalt complex ($K_d(333K) \sim 10^{-10}$). This is illustrated by the parallel linear regions of the first-order rate plots that occur when all of the V-70 radical source has dissociated (Figure 3).

Figure 4 illustrates a representative plot for the measured number-average molecular weight and polydispersity as a

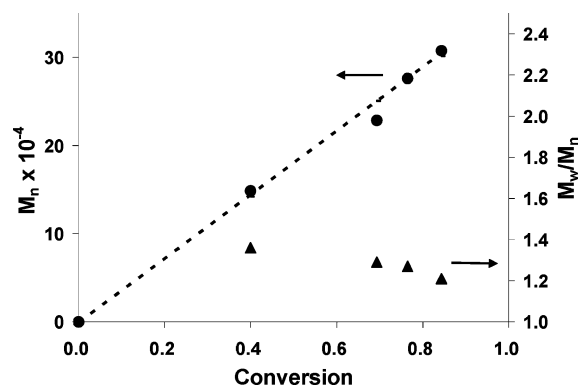


Figure 4. Change in the number-average molecular weight (M_n) and polydispersity (M_w/M_n) with acrylic acid (AA) with conversion of AA to PAA at 333 K. $[AA]_i = 4.72$ M; $[(TMPS)Co^{II}]_i = 1.14 \times 10^{-3}$ M; $[V-70]_i = 1.88 \times 10^{-3}$ M. The dotted line is the theoretical line for one polymer chain per organocobalt complex.

function of monomer conversion for acrylic acid polymerization in the presence of $(TMPS)Co^{II}$ complexes in water. The observed linear increase in number-average molecular weight (M_n) for PAA with conversion of acrylic acid indicates that there is a nearly constant number of chains that are growing at effectively the same rate which is a signature for high living character. The PAA polymers formed are highly linear as evidenced by the inability to detect the ^{13}C NMR resonances in the range ($\delta(^{13}C) = 36-40$ and $47-50$ ppm) that are characteristic of acrylate branching (Figure 5).^{17,29,30} Chain transfer to solvent which could limit polymer growth^{22,25} is also quenched by using aqueous reaction media.

Magnetic anisotropy ring currents of aromatic porphyrin ligands result in high field NMR shifts that scale by $(3 \cos^2\theta - 1)/r^3$ from the center of the ring for magnetic nuclei in groups that are bonded with metal sites in metalloporphyrin. Hydrogen nuclei in organic groups as far as seven bonds away from the metal often have upfield shifts that place the hydrogen resonances in the clear region on the high field side of TMS. 1H NMR thus provides a powerful method to observe the organic units bonded with the metal in organocobalt porphyrin complexes. Figure 6 depicts the time evolution of the 1H NMR in the region on the high field side of TMS ($\delta < 0$) during polymerization of AA (0.073 M), initiated by V-70 (3.37×10^{-3} M) in the presence of $[(TMPS)Co^{II}]^+$ (3.26×10^{-3} M) at 333 K. During the induction period the radicals that enter solution from V-70 ($^{\bullet}C(CH_3)(CN)(C(CH_3)_2OCH_3)$) react at high efficiency with $[(TMPS)Co^{II}]^+$ to form a terminal alkene and a cobalt hydride $((TMPS)Co-H)$ that adds with AA to form $(TMPS)Co-CH(CO_2H)CH_3$ as the initial organometallic species (eq 1–3). The porphyrin pyrrole peak for the paramagnetic $(TMPS)Co^{II}$ complex is shown to disappear during the induction period (Figure 6 inset). Appearance of characteristic doublet methyl ($\delta = -4.91$ ppm) and C–H quartet ($\delta = -3.33$ ppm) resonances demonstrate formation of $(TMPS)Co-CH(CO_2H)-CH_3$. An organometallic species subsequently forms that is assigned as a complex of the AA dimer $((TMPS)Co-CH(CO_2H)CH_2-CH(CO_2H)CH_3)$ based on the high field 1H NMR (Figure 6). The pair of doublet resonances at $\delta = -0.28, -0.84$ ppm are assigned as the terminal methyl group for two diastereomers (*rr*, *ss*; *rs*, *sr*) that arise from the two chiral centers in the AA dimer unit. Near the end of the induction period the AA dimer complex is replaced by organocobalt complexes of AA oligomers $((TMPS)Co-CH(CO_2H)CH_2-CH(CO_2H)-CH_2-PAA)$. 1H NMR from -3 to -5 ppm have the six characteristic resonances for the first AA unit $((TMPS)Co-$

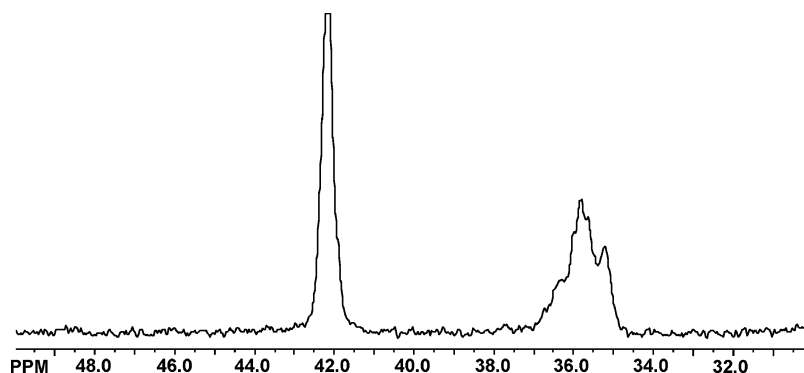
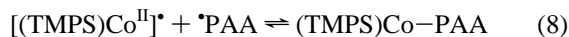
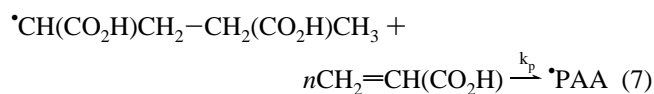
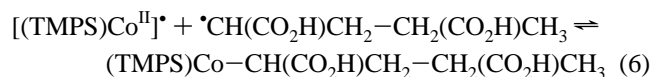
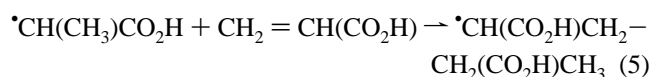
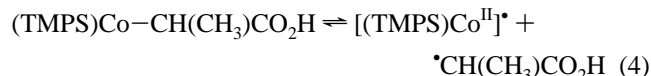
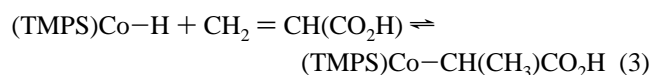
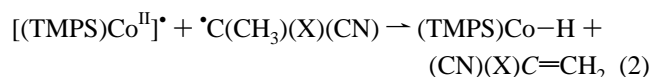
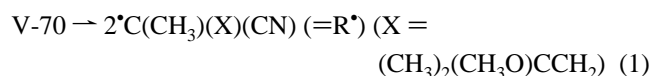


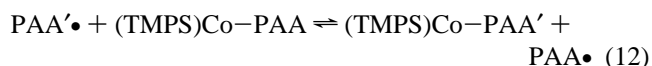
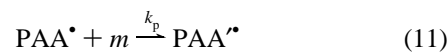
Figure 5. ^{13}C NMR (300 MHz) spectrum in C_6D_6 of polymethyl acrylate (PMA) produced by methylation of poly(acrylic acid) (PAA) that was synthesized by cobalt porphyrin mediated LRP in water (Figure 1A, $M_n = 232\,000$; $M_w/M_n = 1.20$).

$\text{CH}(\text{CO}_2\text{H})\text{CH}_2-$ in two diastereomers. Chirality of the organo groups in $(\text{TMPS})\text{Co}-\text{CH}(\text{CO}_2\text{H})\text{CH}_3$ and $(\text{TMPS})\text{Co}-\text{CH}(\text{CO}_2\text{H})\text{CH}_2-\text{CH}(\text{CO}_2\text{H})\text{CH}_2-\text{PAA}$ also makes the adjacent pyrrole hydrogens diastereotopic and the magnetic anisotropy of the carboxylate groups produces an observed pyrrole AB pattern.



At the end of the induction period effectively all of the $[(\text{TMPS})\text{Co}^{\text{II}}]^\bullet$ is converted to organocobalt complexes of the poly(acrylic acid) radical $((\text{TMPS})\text{Co}-\text{PAA})$. Radicals continue to enter solution from V-70 which in the absence of cobalt(II) trapping react with the AA monomer to initiate radical polymerization (Figure 1–3). A period of fast radical polymerization then occurs in the presence of the cobalt-PAA complex $((\text{TMPS})\text{Co}-\text{PAA})$. The rate of polymerization from the end of the induction period through the stage of rapid polymerization is found to be proportional to the square root of the V-70 concentration $([\text{R}^\bullet] = [(k_i/2k_t)[\text{V-70}]]^{1/2})$ which demonstrates that the external radical source (V-70) determines the radical concentration (Figure 7). Linear growth in molecular weight with conversion, molecular weight corresponding to one growing chain per cobalt, and relatively narrow polydispersity show that the polymerization is well controlled during the period of rapid polymerization (Figure 4).

During the period of rapid polymerization the process must be controlled by the organocobalt complexes through a transition metal degenerative transfer that involves exchange of propagating radicals in solution and the dormant radicals in the organocobalt complexes (eqs 9–12).



After the external radical source is fully reacted ($t > 90$ min, $T = 60^\circ\text{C}$) the system contains a dormant polymer organocobalt complex $((\text{TMPS})\text{Co}-\text{PAA})$. Reversible dissociation of the dormant complex provides a source of polymeric radicals (PAA^\bullet) that are maintained at a relatively low concentration by a quasi-equilibrium (eq 8). Acrylic acid polymerization continues at a lower rate under control by reversible termination of $(\text{TMPS})\text{Co}-\text{PAA}$. Observation of equal slopes for the first-order rate plots at the same concentration of organometallic complex is consistent with this mechanism (Figure 3). The AA polymerization controlled by the reversible termination mechanism attains living character through the persistent radical effect.³¹

At the conditions where organocobalt complexes mediate a degenerative transfer LRP the injection of radicals from an external source (V-70, AIBN) suppresses the cobalt(II) concentration to a sufficiently small concentration such that β -H abstraction from the growing polymeric radical is effectively quenched. The requirement for having sterically demanding complexes as an approach to suppress β -H abstraction from the growing oligomer/polymer radicals is eliminated when the cobalt(II) concentration can be maintained at a sufficiently low level. This important feature is illustrated by the successful use of the lower steric demand organocobalt tetra(4-sulfonatophenyl) porphyrin $(\text{TSPP})\text{Co}-\text{R}$ complexes to mediate a living polymerization of acrylic acid during the time period when radicals from V-70 are entering solution (Figure 8).

The conversion of AA ($[\text{AA}]_i = 4.72$ M) as a function of time at 333 K in water using V-70 ($[\text{V-70}]_i = 5.85 \times 10^{-4}$ M) as the radical source in the absence and presence of organocobalt complexes is illustrated in Figure 9. The use of a preformed organocobalt complex $((\text{TMPS})\text{Co}-\text{CH}(\text{CO}_2\text{H})\text{CH}_3)$ eliminates the induction period observed when $(\text{TMPS})\text{Co}^{\text{II}}$ is the catalyst precursor (Figure 9B). The rate of AA polymerization in the presence of $(\text{TMPS})\text{Co}-\text{PAA}$ is less than when the cobalt

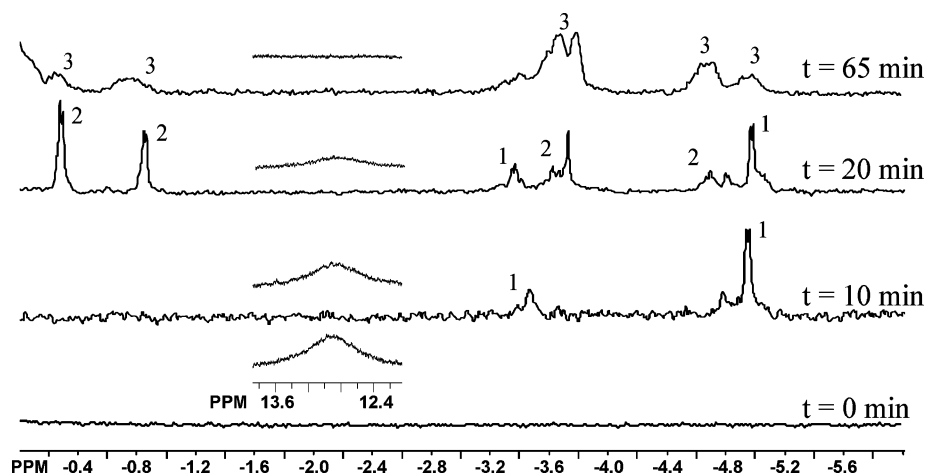


Figure 6. ^1H NMR (300 MHz) illustrating the time evolution of diamagnetic organocobalt complexes during the induction period for the polymerization system consisting of $[\text{AA}]_i = 0.073 \text{ M}$, $[(\text{TMPS})\text{Co}^{\text{II}}]_i = 3.26 \times 10^{-3} \text{ M}$, and $[\text{V-70}]_i = 3.37 \times 10^{-3} \text{ M}$ (D_2O , 333 K). Key: (1) $(\text{TMPS})\text{Co}-\text{CH}(\text{CO}_2\text{H})\text{CH}_3$; (2) $(\text{TMPS})\text{Co}-\text{CH}(\text{CO}_2\text{H})\text{CH}_2-\text{CH}(\text{CO}_2\text{H})\text{CH}_3$; (3) $(\text{TMPS})\text{Co}-\text{PAA}$. **Inset.** The pyrrole resonance for paramagnetic $(\text{TMPS})\text{Co}^{\text{II}}$ disappears during the induction period.

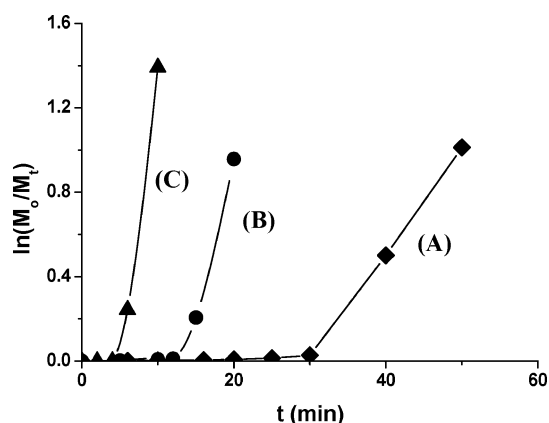


Figure 7. Kinetic plots for polymerization of acrylic acid ($[\text{AA}]_i = 4.72 \text{ M}$) in D_2O at 333 K with $[(\text{TMPS})\text{Co}^{\text{II}}]_i = 1.4(0.02) \times 10^{-3} \text{ M}$ and a series of V-70 concentrations. (A) $[\text{V-70}]_i = 1.05 \times 10^{-3} \text{ M}$; $[\text{V-70}]_i/[(\text{TMPS})\text{Co}^{\text{II}}]_i = 0.80$; conversion = 63.7%; $M_n = 156\,000$ (theory 153 000); $M_w/M_n = 1.22$. (B) $[\text{V-70}]_i = 1.68 \times 10^{-3} \text{ M}$; $[\text{V-70}]_i/[(\text{TMPS})\text{Co}^{\text{II}}]_i = 1.00$; conversion = 61.6%; $M_n = 139\,000$ (theory 148 000); $M_w/M_n = 1.28$. (C) $[\text{V-70}]_i = 2.80 \times 10^{-3} \text{ M}$; $[\text{V-70}]_i/[(\text{TMPS})\text{Co}^{\text{II}}]_i = 2.20$; conversion = 75.1%; $M_n = 206\,000$ (theory 185 000); $M_w/M_n = 1.31$.

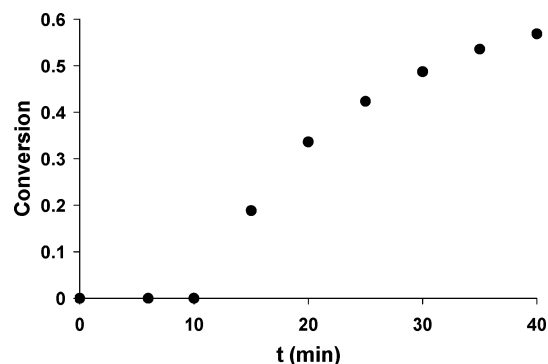


Figure 8. Monomer conversion as a function of time in the radical polymerization of acrylic acid (AA) in D_2O at 333 K initiated by V-70 with $[\text{AA}]_i = 4.72 \text{ M}$; $[(\text{TSP})\text{Co}^{\text{II}}]_i = 1.24 \times 10^{-3} \text{ M}$; $[\text{V-70}]_i = 1.68 \times 10^{-3} \text{ M}$; $[\text{V-70}]_i/[(\text{TSP})\text{Co}^{\text{II}}]_i = 1.35$; conversion = 56.9%; $M_n = 156\,000$ (theory 164 000); $M_w/M_n = 1.37$.

complex is absent (Figure 9). Similar rate decreases were observed in the $(\text{TMP})\text{Co}-\text{PMA}$ initiated polymerization of methyl acrylate (MA) in benzene²⁶ and in polymerizations controlled by RAFT reagents.^{7,15}

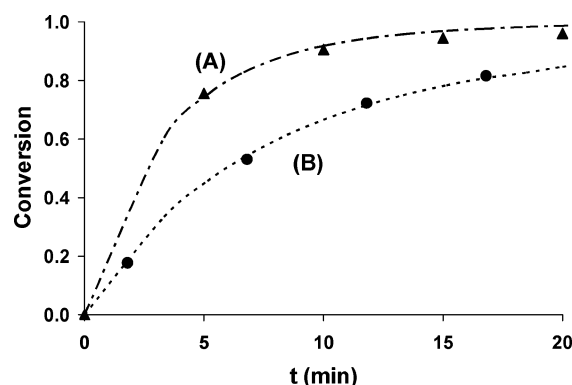


Figure 9. Conversion of acrylic acid (AA) in D_2O as a function of time at 333 K initiated by V-70 with $[\text{AA}]_i = 4.72 \text{ M}$; $[\text{V-70}]_i = 5.85 \times 10^{-4} \text{ M}$. Key: (A) absence of $(\text{TMPS})\text{Co}$ species; (B) $[(\text{TMPS})\text{Co}-\text{CH}(\text{CO}_2\text{H})\text{CH}_3]_i = 1.30 \times 10^{-3} \text{ M}$. Conversion = 81.6%; $M_n = 232\,000$ (theory 212 000); $M_w/M_n = 1.20$. Dashed lines are calculated from kinetic parameters given in the Experimental Section.

Smaller rates of radical polymerization ($-\text{d}[\text{m}]/\text{d}t = k_p[\text{R}^*][\text{m}]$) in the presence of $(\text{TMPS})\text{Co}-\text{PAA}$ implies that the radical concentration ($[\text{R}^*] = [(k_i/2k_t)[\text{V-70}]]^{1/2}$) from V-70 is reduced by the presence of $(\text{TMPS})\text{Co}-\text{PAA}$. The rate of radicals entering solution from V-70 ($\text{d}[\text{R}^*]/\text{d}t = k_i[\text{V-70}]/2k_t$) is the same in the presence and absence of $(\text{TMPS})\text{Co}-\text{PAA}$ and thus the decrease in effective radical concentration must result from an increase in the effective radical termination constant (k_t) when $(\text{TMPS})\text{Co}$ species are present. One possible reason for a larger effective k_t associated with the presence of $(\text{TMPS})\text{Co}-\text{PAA}$ is that the average polymer chain length is smaller for the controlled LRP process.

Summary

Water-soluble cobalt(II) porphyrins in conjunction with an azo radical source and acrylic acid form organocobalt complexes that mediate a living radical polymerization of AA in water. Low polydispersity high molecular weight poly(acrylic acid) is rapidly formed by the aqueous polymerization system. Linear increase in number-average molecular weight with monomer conversion and relatively low polydispersity indicate the living character of polymerization. Kinetic-mechanistic studies demonstrate that when an external radical source like V-70 injects radicals into solution organocobalt complexes mediate a rapid living radical polymerization that occurs by a degenerative

transfer radical interchange polymerization (RIP) mechanism.

Experimental Section

Materials. Acrylic acid (Sigma-Aldrich, 99%, 200 ppm MEHQ inhibitor) was stored at room temperature and vacuum distilled before use. The azo initiator, V-70 ($[(\text{CH}_3)_2\text{CH}_2\text{O}]\text{C}(\text{CH}_3)_2\text{N}_2$), was purchased from Wako Chemicals Inc. and recrystallized using methanol. Cobalt acetate (97%) was supplied by Fisher Scientific and used as received. The methylation agent, trimethylsilyldiazomethane (2 M solution in diethyl ether), was purchased from Aldrich. Solutions of AA, TMPS, and V-70 were subjected to three freeze–pump–thaw cycles to remove any residual oxygen.

Analytical Techniques. Identification of organocobalt porphyrin complexes, monomer conversion, and porphyrin structure were evaluated by ^1H NMR using a Bruker AC-360 interfaced to an Aspect 300 computer at ambient temperature. Chemical shifts were calibrated on the basis of the solvent peak (deuterated water at 4.80 ppm, purchased from Cambridge Isotope Laboratory Inc.). The percent conversion was determined by integrating the resonances corresponding to the vinyl protons of the monomer (5.5–6.3 ppm) and aliphatic protons of the polymer (0.6–2.3 ppm).

Gel permeation chromatography (GPC) analysis for PAA was made on a Shimadzu modular system, comprised of a Polymer Laboratories 5.0 μm PLgel guard column (50×7.5 mm) followed by three linear PLgel columns (10^6 , 10^4 , and 5×10^2 Å) in an oven (CTO-10A), a UV detector (SPD-10AV) at 600 nm and a differential refractive index detector (RID-10A), using tetrahydrofuran (THF) as the eluent at 40 °C with a flow rate of 1 mL min^{-1} was used. This system was calibrated using narrow peak width polystyrene standards (Easical, pre-prepared polymer calibrants purchased from Polymer Laboratories) ranging from 580 to 7.5 $\times 10^6$ g mol^{-1} .

Preparation of $\text{Na}_8(\text{TMPS})\text{H}_2$. Tetrakis(3,5-disulfonatomesityl)porphyrin (TMPS) was synthesized according to modified literature methods.³³ Tetramesitylporphyrin³⁴ (20 mg) was placed in a round-bottom flask, and 0.1 mL of fuming sulfuric acid $\text{SO}_3 \cdot x\text{H}_2\text{SO}_4$ (purchased from Aldrich) was carefully added dropwise. The solution became green immediately and was stirred for 2 h in a 90.0 °C oil bath sealed with a septum. After the reaction was complete, the flask was cooled using an ice bath and the solution was added dropwise into 20 mL of pure water. Aqueous sodium hydroxide (2.0 M) was used to neutralize the excess acid to pH of 7. The product was extracted using methanol and further purified using silica chromatography with methanol as the eluent (yield 68–77%). ^1H NMR (D_2O): δ (ppm): 8.80 (br, 8H, pyrrole *H*), 3.18 (s, 12H, *p*- CH_3), 2.10 (s, 24H, *o*- CH_3); UV–vis (H_2O): λ_{max} = Soret 418 nm; Q bands 520, 554, 590, 646 nm.

Preparation of $(\text{TMPS})\text{Co}^{\text{II}}$. Methanol solutions of TMPS (2.0 mL of 2.60×10^{-3} M) were mixed with aqueous cobalt acetate (0.2 mL of 3.0×10^{-2} M) and methanol (1.8 mL) in a round-bottom flask under a nitrogen atmosphere. The solution was stirred overnight in a 90.0 °C oil bath sealed with a septum. After the reaction was complete, this solution was used as stock solution. Because of the air sensitivity of $(\text{TMPS})\text{Co}^{\text{II}}$ in water, the stock solution was kept in an inert atmosphere box. (yield 83–90%). ^1H NMR (D_2O): δ (ppm): 12.95 (br, 8H, pyrrole *H*), 3.70 (s, 12H, *p*- CH_3), 2.00 (s, 24H, *o*- CH_3).

Polymerization Procedures. Quantitative stock solutions of $(\text{TMPS})\text{Co}^{\text{II}}$ and acrylic acid in D_2O and V-70 in dichloromethane were prepared in an inert atmosphere box. Aliquots of the $(\text{TMPS})\text{Co}^{\text{II}}$ and V-70 solutions were mixed to obtain desired ratios of V-70 to $(\text{TMPS})\text{Co}^{\text{II}}$ in a vacuum adapted NMR tube and the solvents were subsequently fully removed under vacuum. A measured volume of the D_2O stock solution of AA was then injected into the vacuum-adapted tube containing $(\text{TMPS})\text{Co}^{\text{II}}$ and V-70 and subjected to three freeze–pump–thaw cycles to remove dissolved gases. The reaction tube and sample were then placed in a constant temperature bath (60.0 \pm 0.1 °C) and the progress of the polymerization followed by ^1H NMR.

One specific polymerization sample was prepared by mixing a $(\text{TMPS})\text{Co}^{\text{II}}$ solution (0.20 mL of 2.60×10^{-3} M) and V-70 (0.16 mL of 4.21×10^{-3} M) in dichloromethane in a vacuum adapted NMR tube. Subsequent to removing the solvents, 0.40 mL of a 4.72 M D_2O solution of acrylic acid was injected into the NMR tube and subjected to three freeze–pump–thaw cycles. The sample was placed in a 60.0 °C constant temperature bath and the polymerization followed by ^1H NMR. Monomer conversion reached 81.6% in 30 min and the number-average molecular weight of the polymeric products were 233 000 (theory 212 000) with polydispersity of 1.20 (Figure 1A). The polymer products were transferred from the reaction tube to the round-bottom flasks using methanol. The solvent was then removed under vacuum and the dried polymer products were dissolved in a methanol THF mixture solution and methylated for the GPC analysis without further purification.

Methylation of PAA. The acrylic acid polymers were modified by methylation of the carboxylic acid groups using trimethylsilyldiazomethane for GPC measurement using THF as the solvent.^{35,25} The PAA samples were dissolved in a mixture of THF and methanol. The methylation agent was added dropwise into the polymer solution. Upon addition, bubbles appeared, and the color of the solution changed from red-orange to yellow-green. Addition of methylation agent was continued until the solution became yellow-green and ceased bubbling. This solution was stirred for 2 h at room temperature and then dried by vacuum. Proton NMR spectroscopy confirmed that the methylation to form polymethyl acrylate was essentially quantitative.

Kinetic Simulations. The simulation program, MacKinetics v0.9.1, was generously provided by Dr. Walter S. Leipold III. The following equations and rate constants are used for kinetic simulation. The rate



constant for V-70 decomposition (k_{act}) is calculated from tables provided by Wako Chemicals (eq 13). The radical initiator efficiency ($0.62 = k_d(1)/[k_d(1) + k_t(1)]$) was measured by a chemical trapping method.³⁶ The rate of radicals entering solution ($d[\text{R}^{\bullet}]/dt$) is equal to 1.24 times the rate of decomposition of V-70 ($-d[\text{V-70}]/dt$). The propagation rate constant (k_p) for acrylic acid as a function of temperature and concentration were obtained from published data of I. Lacik (eq 16).²⁸ The equilibrium constant ($k_d(2)/k_a$, 1.0×10^{-10}) was determined by the results of the kinetic studies for LRP mediated by TMPSCo . The termination rate constant ($k_t(2)$) is varied to obtain the best fit with the experimental measurements.

Acknowledgment. This research was supported by Grant NSF–CHE-0501198.

References and Notes

- (1) (a) Matyjaszewski, K. Ed. *Advances in Controlled/Living Radical Polymerization*; ACS Symposium Series 854; American Chemical Society: Washington, DC, 2003. (b) Matyjaszewski, K.; Ed. *Controlled/Living Radical Polymerization: From Synthesis to Materials*; ACS Symposium Series 944; American Chemical Society: Washington, DC, 2006.

- (2) Georges, M. K.; Veregin, R. P. N.; Kazmaier, P. M.; Hamer, G. K. *Macromolecules* **1993**, *26*, 2987–2988.
- (3) Wayland, B. B.; Poszmik, G.; Mukerjee, S. L.; Fryd, M. *J. Am. Chem. Soc.* **1994**, *116*, 7943–7944.
- (4) Kato, M.; Kamigaito, M.; Sawamoto, M.; Higashimura, T. *Macromolecules* **1995**, *28*, 1721–1723.
- (5) Wang, J. S.; Matyjaszewski, K. *J. Am. Chem. Soc.* **1995**, *117*, 5614–5615.
- (6) Percec, V.; Barboiu, B. *Macromolecules* **1995**, *28*, 7970–7972.
- (7) Chiefari, J.; Chong, Y. K.; Ercole, F.; Krstina, J.; Jeffery, J.; Le, T. P. T.; Mayadunne, R. T. A.; Meijs, G. F.; Moad, C. L.; Moad, G.; Rizzardo, E.; Thang, S. H. *Macromolecules* **1998**, *31*, 5559–5562.
- (8) Fukuda, T.; Goto, A. *Macromol. Rapid Commun.* **1997**, *18*, 683–688.
- (9) Asandei, A. D.; Moran, I. W. *J. Am. Chem. Soc.* **2004**, *126*, 15932–15933.
- (10) Debuigne, A.; Caille, J.-R.; Jèrôme, R. *Angew. Chem., Int. Ed.* **2005**, *44*, 1101–1104.
- (11) Poli, R. *Angew. Chem., Int. Ed.* **2006**, *45*, 5058–5070.
- (12) Matyjaszewski, K.; Xia, J. H. *Chem. Rev.* **2001**, *101*, 2921–2990.
- (13) Kamigaito, M.; Ando, T.; Sawamoto, M. *Chem. Rev.* **2001**, *101*, 3689–3746.
- (14) Hawker, C. J.; Bosman, A. W.; Harth, E. *Chem. Rev.* **2001**, *101*, 3661–3688.
- (15) Moad, G.; Rizzardo, E.; Thang, S. H. *Aust. J. Chem.* **2005**, *58*, 379–410.
- (16) Asandei, A. D.; Moran, I. W.; Saha, G.; Chen, Y. *J. Polym. Sci., Part A: Polym. Chem.* **2006**, *44*, 2156–2165.
- (17) Kwak, Y.; Goto, A.; Fukuda, T.; Kobayashi, Y.; Yamago, S. *Macromolecules* **2006**, *39*, 4671–4679.
- (18) Bryaskova, R.; Detrembleur, C.; Debuigne, A.; Jèrôme, R. *Macromolecules* **2006**, *39*, 8263–8268.
- (19) Percec, V.; Guliasvili, T.; Ladislav, J. S.; Wistrand, A.; Stjerndahl, A.; Sienkowska, M. J.; Monteiro, M. J.; Sahoo, S. *J. Am. Chem. Soc.* **2006**, *128*, 14156–14165.
- (20) Maria, S.; Kaneyoshi, H.; Matyjaszewski, K.; Poli, R. *Chem.—Eur. J.* **2007**, *13*, 2480–2492.
- (21) Patten, T. E.; Matyjaszewski, K. *Adv. Mater.* **1998**, *10*, 901–915.
- (22) Loiseau, J.; Doerr, N.; Suau, J. M.; Egraz, J. B.; Llauro, M. F.; Ladaviere, C.; Claverie, J. *Macromolecules* **2003**, *36*, 3066–3077.
- (23) Ladaviere, C.; Dorr, N.; Claverie, J. P. *Macromolecules* **2001**, *34*, 5370–5372.
- (24) Couvreur, L.; Charleux, B.; Guerret, O.; Magnet, S. *Macromol. Chem. Phys.* **2003**, *204*, 2055–2063.
- (25) Couvreur, L.; Lefay, C.; Belleney, J.; Charleux, B.; Guerret, O.; Magnet, S. *Macromolecules* **2003**, *36*, 8260–8267.
- (26) Wayland, B. B.; Peng, C. -H.; Fu, X.; Lu, Z.; Fryd, M. *Macromolecules* **2006**, *39*, 8219–8222.
- (27) (a) Table of Azo Polymerization initiators provided by Wako Chemicals U.S.A., Inc. (b) Dixon, K. W. In *Polymer Handbook*, 4th ed.; Brandrup, J., Immergut, E. H., Grulke, E. A., Ed.; Wiley: New York, 1999; p II/1.
- (28) Lacik, I.; Beuermann, S.; Buback, M. *Macromolecules* **2001**, *34*, 6224–6228.
- (29) Farcet, C.; Belleney, J.; Charleux, B.; Pirri, R. *Macromolecules* **2002**, *35*, 4912–4918.
- (30) Ahmad, N. M.; Heatley, F.; Lovell, P. A. *Macromolecules* **1998**, *31*, 2822–2827.
- (31) Fischer, H. *Chem. Rev.* **2001**, *101*, 3581–3610.
- (32) Theis, A.; Feldermann, A.; Charton, N.; Stenzel, M. H.; Davis, T. P.; Barner-Kowollik, C. *Macromolecules* **2005**, *38*, 2595–2605.
- (33) Song, R.; Robert, A.; Bernadou, J.; Meunier, B. *Inorg. Chim. Acta* **1998**, *272*, 228–234.
- (34) Lindsey, J. S.; Wagner, R. W. *J. Org. Chem.* **1989**, *54*, 828–836.
- (35) Graham, S.; Cormack, P. A. G.; Sherrington, D. C. *Macromolecules* **2005**, *38*, 86–90.
- (36) Woska, D. C.; Xie, Z. D.; Gridnev, A. A.; Ittel, S. D.; Fryd, M.; Wayland, B. B. *J. Am. Chem. Soc.* **1996**, *118*, 9102–9109.

MA070836N